Journal of Traffic and Transportation Engineering 6 (2018) 155-163
doi: 10.17265/2328-2142/2018.04.001

Aerodynamic Simulation of a 2017 F1 Car with Open-Source CFD Code

Umberto Ravelli and Marco Savini

Department of Engineering and Applied Sciences, University of Bergamo, Dalmine 24044, Italy

Abstract: Open-wheeled race car aerodynamics is unquestionably challenging insofar as it involves many physical phenomena, such as slender and blunt body aerodynamics, ground effect, vortex management and interaction between different sophisticated aero devices. In the current work, a 2017 F1 car aerodynamics has been investigated from a numerical point of view by using an open-source code. The vehicle project was developed by PERRINN (Copyright©2011—Present PERRINN), an engineering community founded by Nicolas Perrin in 2011. The racing car performance is quantitatively evaluated in terms of drag, downforce, efficiency and front balance. The goals of the present CFD (computational fluid dynamics)-based research are the following: analyzing the capabilities of the open-source software OpenFOAM in dealing with complex meshes and external aerodynamics calculation, and developing a reliable workflow from CAD (computer aided design) model to the post-processing of the results, in order to meet production demands.

Key words: External aerodynamics, open-source CFD, 2017 F1 car, drag, downforce, efficiency, front balance.

1. Introduction

Nowadays CFD (computational fluid dynamics) and Motorsport are closely connected and interdependent: on the one hand, aerodynamic simulations are crucial for designing and developing increasingly fast vehicles; on the other hand, the extreme research of performance in motor racing is the catalyst behind the development of sophisticated and reliable numerical procedures and innovative CAE (computer aided engineering) tools.

The impact of CFD on motorsport has grown up in tandem with computer hardware advances: looking at the Formula 1 experience during the period from 1990 to 2010, simulations evolved from the inviscid panel method to one billion cell calculations of entire cars, including analysis of transient behaviour and overtaking [1]. As witnessed by the Formula 1 team Sauber Petronas, the CFD technology is applied in many stages of the vehicle development: early concept phase, system design (engine and brake cooling, brake systems), single component design and complete system design and interactions [2]. Although open-wheeled racing car aerodynamics is basically an unusual field of research, there are a few publications from academic world as well as private industries: as an example of partnership between university and motorsport teams, Zhang, Toet and Zerihan [3] reviewed the progress made during the last 30 years on ground effect aerodynamics.

From the point of view of the required computational resources, the complexity of the geometry and the resulting numerical issues, the simulation of realistic open-wheeled cars is really challenging: for this reason, F1 teams and researchers often rely on commercial software that provide user-friendliness, flexibility and reliability: the more you spend time on pre-processing and debugging, the lesser you can focus on design and physics comprehension. Examples of this type of study can be found in Refs. [4] and [5]: ANSYS software package is used to investigate the impact of 2009 FIA technical regulations on the aerodynamic performance of F1 cars.

Corresponding author: Umberto Ravelli, Ph.D. student, research fields: aerodynamics, F1 car, CFD, OpenFOAM.

In addition to CFD commercial solutions, there are open-source codes able to execute both the meshing phase and the fluid dynamic calculation: one of the most popular is OpenFOAM®. This free-license tool is successfully used and developed by academic researchers [6] and automotive industries [7] in order to predict the aerodynamic performance of road cars; however, due to some criticalities connected to meshing accuracy and numerical stability, it is not widespread in high level motorsport applications. In the current study, the highly complex aerodynamics of a 2017 F1 car has been numerically investigated by OpenFOAM®. Prediction reliability has been tested against reference data of drag, downforce, efficiency and front balance, provided by PERRINN.

2. CFD Workflow: Software and Hardware Tools

The first step of this study consists of developing a standard and reliable CFD workflow (from meshing to calculation) for external aerodynamic analysis of very complex geometries, through the use of the open-source software OpenFOAM. Many degrees of freedom are available in the case setup: the user can decide time and space discretization schemes of the Navier-Stokes equation terms as well as the solver for each variable [8].

The volume mesh is performed by SnappyHexMesh, an OpenFOAM utility providing a non-graphical, fast and flexible procedure for every kind of geometry, especially in external aerodynamics applications. This implies a huge time and resource saving in comparison with a traditional meshing software without a batch mesh utility. On the other hand, it is less accurate than some commercial meshing software, for instance in adding layers and tracing the edges of complex surfaces [8].

Both the meshing and the calculations were carried out using Galileo, the Italian Tier-1 cluster for industrial and public research, available at CINECA SCAI (supercomputing applications and innovations). The meshing processes were executed by means of 6 computational nodes, each of which is composed of 16 cores (8 GB/core); the calculations were instead performed using 14 nodes. About 1,500 iterations were required to get convergence on the basis of residuals lower than 10^{-4}.

3. Pre-processing and Numerical Setup

3.1 Geometry

The input file of the geometry must be in STereoLithography format (stl). Many commercial CAD softwares are able to convert the original model in this format, but it is preferable to use only those providing a detailed control on the output file, since the quality of the stl model is directly connected to the quality of the volume mesh and the accuracy of the final fluid dynamic results.

A final check of the .stl file is recommended in order to control orientation, closure of the surfaces, quality of triangles and edges: Netfabb Basic, a free software, was used in the current study.

The stl file of the F1 car, obtained from the original project by PERRINN (Fig. 1), contains a lot of interesting features and challenges from the perspective of meshing. The full-scale F1 car model, whose wheelbase (*WB*) is 3.475 m long, presents many small realistic details such as winglets, fences, vortex generators and slots: the smallest elements are 1.5 mm thick.

Proximity problems can be found among the suspension arms, the front wing flaps and between the underbody and the ground: with the baseline setup (front ride height = 20 mm; rear ride height = 50 mm), the minimum distance between the plank and the ground is 13 mm. A contact patch between the tires and the ground, established by the front and rear ride height of the vehicle, needs to be defined in order to avoid problems of cell skewness.

Before starting the meshing phase with SnappyHexMesh, the car model is divided into components, so as to analyse separately the behaviour

Fig. 1 Rendering of the 2017 F1 car by PERRINN (image from gpupdate.net).

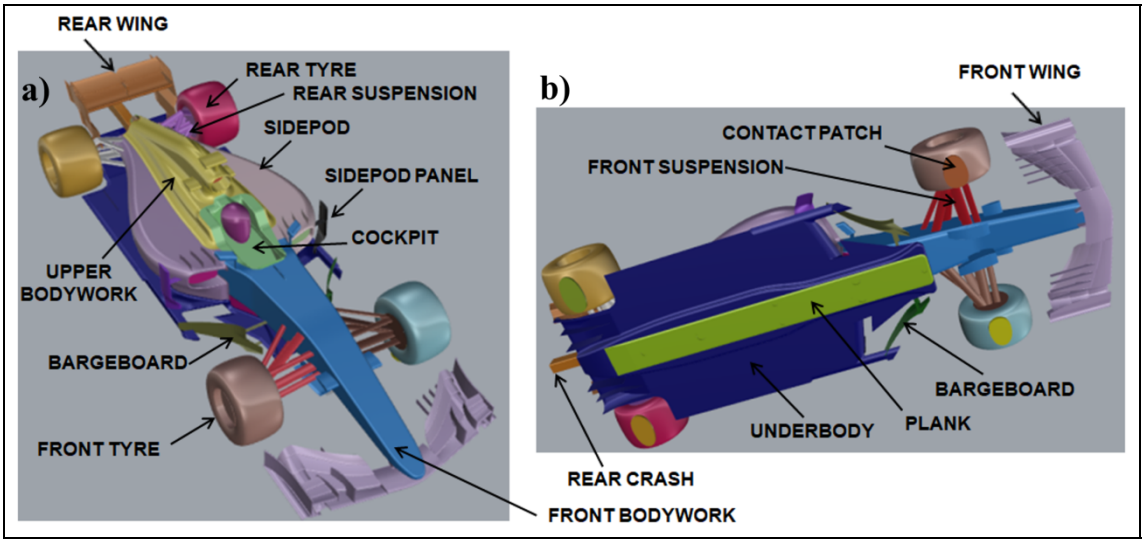

Fig. 2 Geometry in stl format: (a) top view; (b) bottom view.

of each part of the car body (Fig. 2).

3.2 Mesh and Simulation Setup

The domain length is about 18 times the *WB* of the vehicle: the distance between the inlet and the front axle is about 4.6 times the *WB*, while the outlet of the virtual tunnel, where the atmospheric pressure is imposed, is located well downstream of the car, i.e. 13.8 times the *WB* (Fig. 3). Since the simulation is steady and the vehicle is perfectly symmetrical, only half car is taken into account: the distance between the longitudinal symmetry plane and the sidewall is about 16 times the half-width of the car. The height of the domain is 16 times the height (h) of the vehicle. Slip condition is imposed on the side wall and the ceiling of the wind tunnel, while the ground is moving at the same speed imposed at the inlet, for the purpose of comparison with the reference calculation made by PERRINN. Angular velocity and rotational axis of the wheels need to be defined.

The main features of the mesh are as follows: the height of the first cell at all solid surfaces is 0.6 mm and the layer expansion ratio is 1.2. The resulting average value of y^+ is about 40: this number obliges to use wall functions, as is currently done in industrial applications.

Due to the complexity of the geometry and the related physical phenomena, many refinement boxes need to be defined. Special attention must be given to the huge wake region and the parts responsible for

downforce: the multi-component ground effect front wing, the rear wing composed of a high-cambered main plane and a high angle-of-attack flap, and finally the underbody, where the flow reaches its highest velocity.

As suggested by preliminary study [8], two turbulence models were taken into account: the kOmegaSST (kωSST) and the SpalartAllmaras (S-A). Physical data needed to define the numerical setup and initialize the turbulent variables of both simulations are summarized in Table 1. The car *WB*, representing the size of the largest eddy, was chosen as turbulent length scale. The incompressible RANS simulations were performed by the coupled version of the simpleFoam algorithm, which is faster and more stable than the segregated one, at the cost of more computational resources. The GAMG (geometric algebraic multi grid) solver was used for the pressure equation, whilst smoothSolver was applied for velocity and turbulent variables. The entire calculation was executed with 2nd order discretization schemes. Convergence was considered to be reached whenever the scaled pressure and velocity residuals were lower than 10^{-4} and the aerodynamic coefficients remained stable (± 1% in the last 500 iterations).

Three different meshes were tested (140 mln, 120 mln, 90 mln cells): since the results in terms of global performance did not change significantly, the coarsest one was chosen for the research.

4. Results and Discussion

The comparison between numerical predictions and reference data from PERRINN database deals with drag (*SCx*), downforce (*SCz*), aerodynamic efficiency (*Cz/Cx*) and front balance (*FB*), where *S* is the frontal area of the car and *FB* is the ratio between the downforce on the front axle and the total downforce.

The kωSST turbulence model predicted a premature separation of the flow on the suction side of the wings and along the diffuser: as a result, both downforce and drag coefficients were underestimated respectively by 20% and 11%.

On the opposite, S-A showed a better behaviour for boundary layer in adverse pressure gradient [8]: as summarized in Table 2, the results of the coupled RANS simulation with S-A model are consistent with the reference data. The percentage errors in prediction of drag and downforce are respectively 6% and 7%, whilst the front balance coefficient differs by 10% from reference datum. After proper validation, Table 3 summarizes the contribution of the main vehicle components to the vertical load (*SCz*). The bottom of the car, composed of the underbody and the plank, generates more or less the 58% of the overall downforce, whilst the front and the rear wing provide respectively the 26.3% and the 27.5% of the total contribution. Also the front bodywork has a beneficial effect in terms of downforce; on the contrary, sidepod

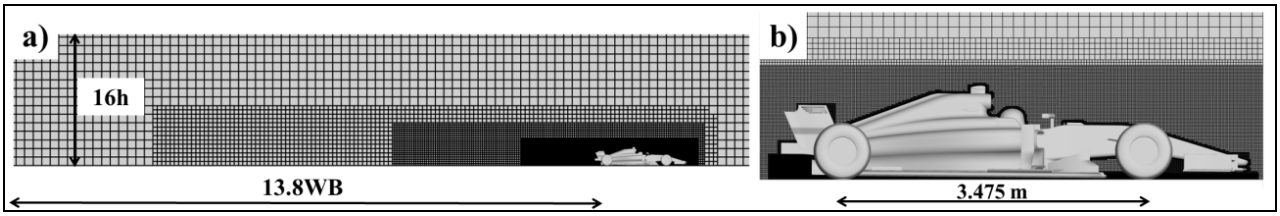

Fig. 3 Volume mesh: (a) symmetry plane; (b) details of the refinement boxes around the car.

Table 1 Physical conditions of the simulation.

Variable	Value
Freestream velocity (u_∞)	50 m/s
Air density (ρ)	1.225 kg/m^3
Turbulent intensity (I)	0.15%
Wheelbase of the vehicle (WB)	3.475 m
Reynolds Number (Re_{WB})	12×10^6

Table 2 Comparison between numerical results and reference data (S-A model).

	SCx [m^2]	*SCz* [m^2]	*Cz*/*Cx*	*FB*
Reference data	1.23	-3.59	2.92	0.448
S-A results	1.16	-3.35	2.89	0.403
Error %	5.7	6.7	1.0	10.0

Table 3 Contribution to downforce of the main components of the car.

Component	*SCz* [m^2]	Contribution (%)
Cockpit	+0.04	+1.2
Driver	+0.02	+0.6
Front bodywork	-0.10	-3.0
Front suspension	+0.06	+1.8
Front wing	-0.88	-26.3
Plank	-0.45	-13.4
Rear suspension	-0.01	-0.3
Rear wing	-0.92	-27.5
Sidepod	+0.2	+6.0
Underbody	-1.49	-44.5
Upper bodywork	+0.18	+5.4
Full car	-3.35	≈-100

Table 4 Contribution to drag of the main components of the car.

Component	*SCx* [m^2]	Contribution (%)
Front tire	+0.115	+9.9
Rear tire	+0.226	+19.5
Front bodywork	+0.055	+4.7
Front suspension	+0.012	+1.0
Front wing	+0.159	+13.7
Rear suspension	+0.024	+2.1
Rear wing	+0.235	+20.3
Sidepod	+0.035	+3.0
Underbody	+0.181	+15.6
Upper bodywork	+0.021	+1.8
Bargeboard	+0.047	+4.1
Other parts	+0.05	+4.3
Full car	+1.16	≈ -100

and upper bodywork generate undesirable lift because they deflect the flow downwards.

Concerning *SCx*, one can see in Table 4 that wheels are responsible for approximately 30% of total drag.

The underbody is the most efficient aerodynamic device, because it makes extensive use of ground effect and Venturi effect to generate downforce, in contrast to rear wing. Despite the complexity of the suspension geometry, its contribution to drag is only 3%, owing to the fact that arm sections are streamlined like a wing profile.

Fig. 4 illustrates the pressure coefficient (C_P) on the surface of the car. The bottom of the bodywork is characterized by typical low-pressure cores which are located at the beginning of the plank, where the ground clearance is smallest, at the entrance of underbody and rear diffuser. In close proximity to the rear tire disturbance, the pressure increases and the ground effect benefits are lost. The upper view shows the contribution to downforce of the front bodywork, due to the shape of the nose cone and the stagnation area in front of the cockpit. As regards the wings, it

can be noted that the rear wing generates downforce mainly due to the high camber of the airfoil design; on the contrary the front wing makes use of ground effect to accelerate the flow on the suction side.

Both generation of downforce and induced drag are strictly connected with the management of axial vorticity: an overall view of these three-dimensional rotational structures can be identified by the iso-surface of the scalar Q [1/s^2]: this variable, defined as the second invariant of the velocity gradient tensor, allows detection of the regions where the Euclidian norm of the vorticity tensor prevails over that of the rate of strain [9].

As illustrated in Fig. 5, the front wing generates not only downforce but also vortices that bypass the front tires. The bargeboard, apart from shielding the underbody from the tire wake, generates a pair of counter-rotating vortices: the upper one travels down the sidepod and acts as an aerodynamic skirt, sealing the low-pressure area under the underbody; the lower

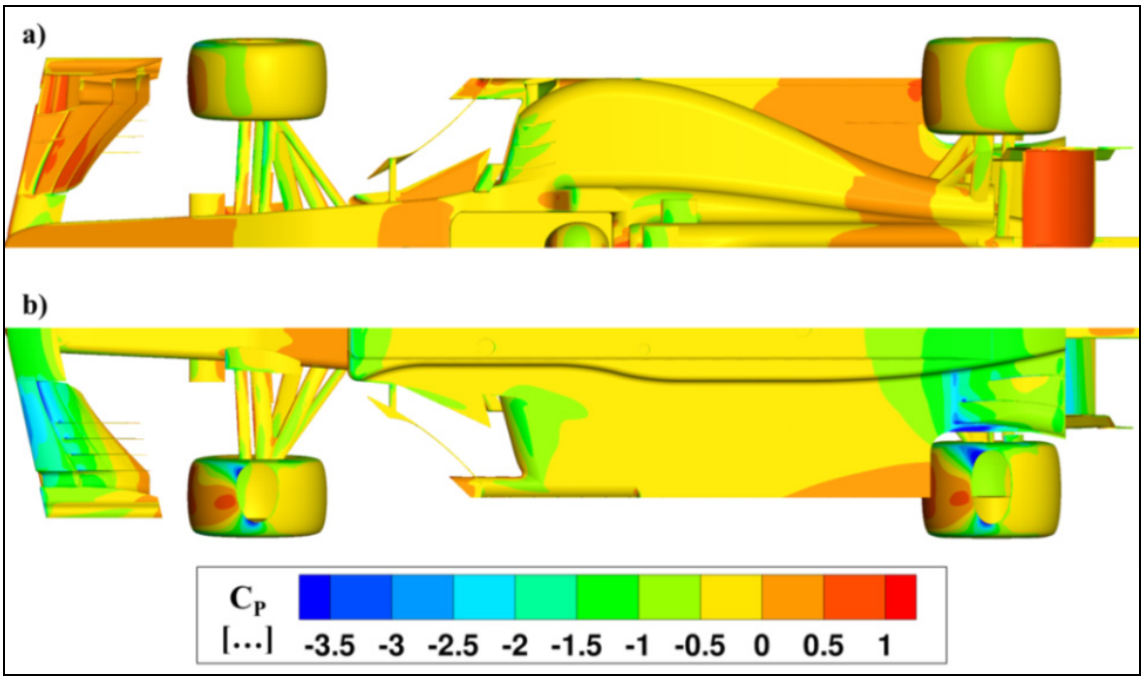

Fig. 4 Pressure coefficient contours: (a) top view; (b) bottom view.

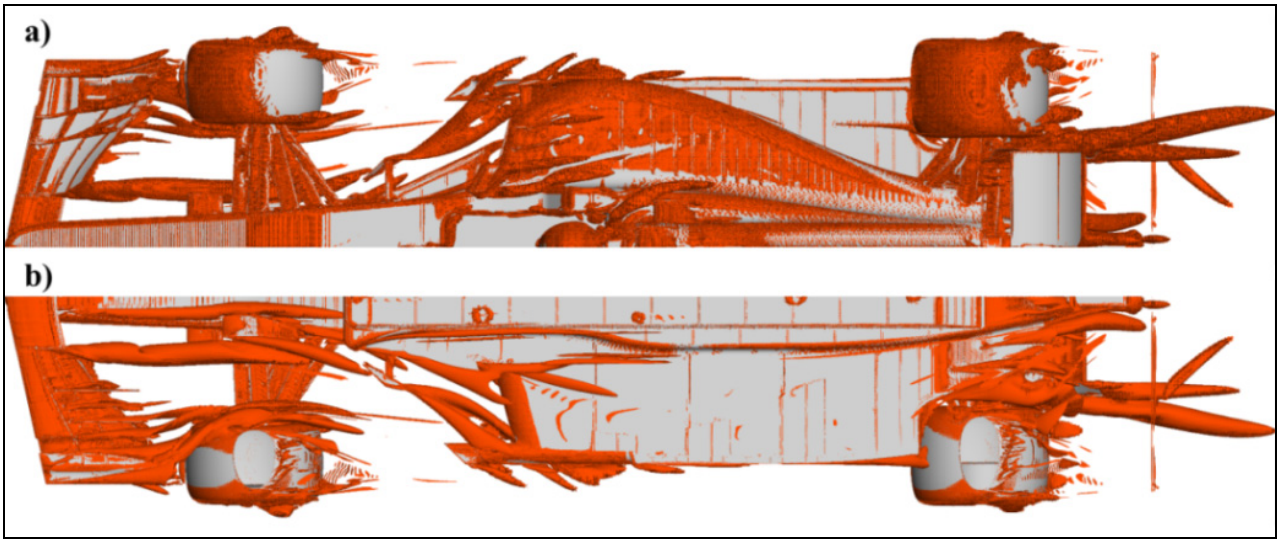

Fig. 5 Iso-contour of Q = 50,000 1/s^2: (a) top view; (b) bottom view.

vortex energizes the flow at the bottom of the car.

Looking at the rear part of the vehicle, one can see the Venturi vortex developing at the inlet of the diffuser due to the difference of pressure between the underbody and the region at the side of the diffuser itself. Finally, the typical wingtip vortices detach from the rear wing, despite the presence of endplates and slots.

Further details about the vortical structures around the single components of the vehicle bodywork can be examined by plotting axial vorticity contours. Fig. 6a clearly shows the presence of the so called Y250 vortex: it develops between the neutral middle section and remaining profiles of the front wing and governs the flow towards the underbody inlet. The outwash endplate and the channel underneath the end of the wing (called Venturi channel) generate a couple of vortices, with negative vorticity, which help the flow to bypass the front tire. The interaction between the front wing and the front tire represents a really complex phenomenon due the unsteadiness of the flow and the influence of the tire alignment parameters (camber, steering angle and toe angle) on vortex development. Fig. 6b shows three main vortex cores: as mentioned before, two of them are related to the bargeboard; the third one, located between the bargeboard itself and the plank, is generated by the delta-shaped part of the underbody. As witnessed by Fig. 6c, the vortex tubes develop along the entire step plane: the low pressure core of these fluid dynamic structures contributes to generation of downforce, in absence of side skirts that isolate the underbody flow.

Concerning the rear region of the car (Fig. 6d), one can see the two vortices generated by the diffuser fences into the side of the main Venturi vortex. Looking at the flow underneath the car, each main vortex is coupled with a secondary structure, because of its interaction with the ground boundary layer.

For the purpose of concluding the qualitative analysis of the flow, streamlines around the main components of the vehicle are plotted in Fig. 7. The dual

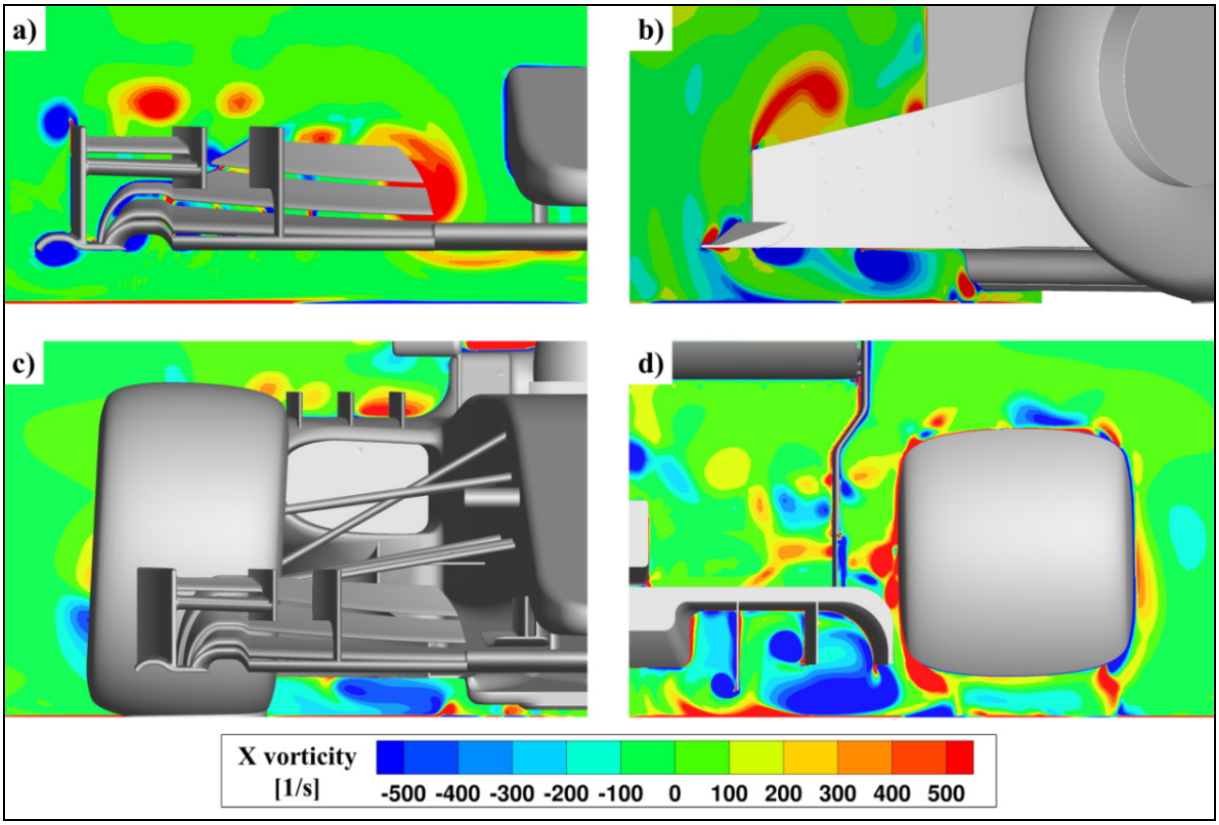

Fig. 6 Axial vorticity contours: (a) front wing; (b) bargeboard; (c) middle underbody; (d) diffuser.

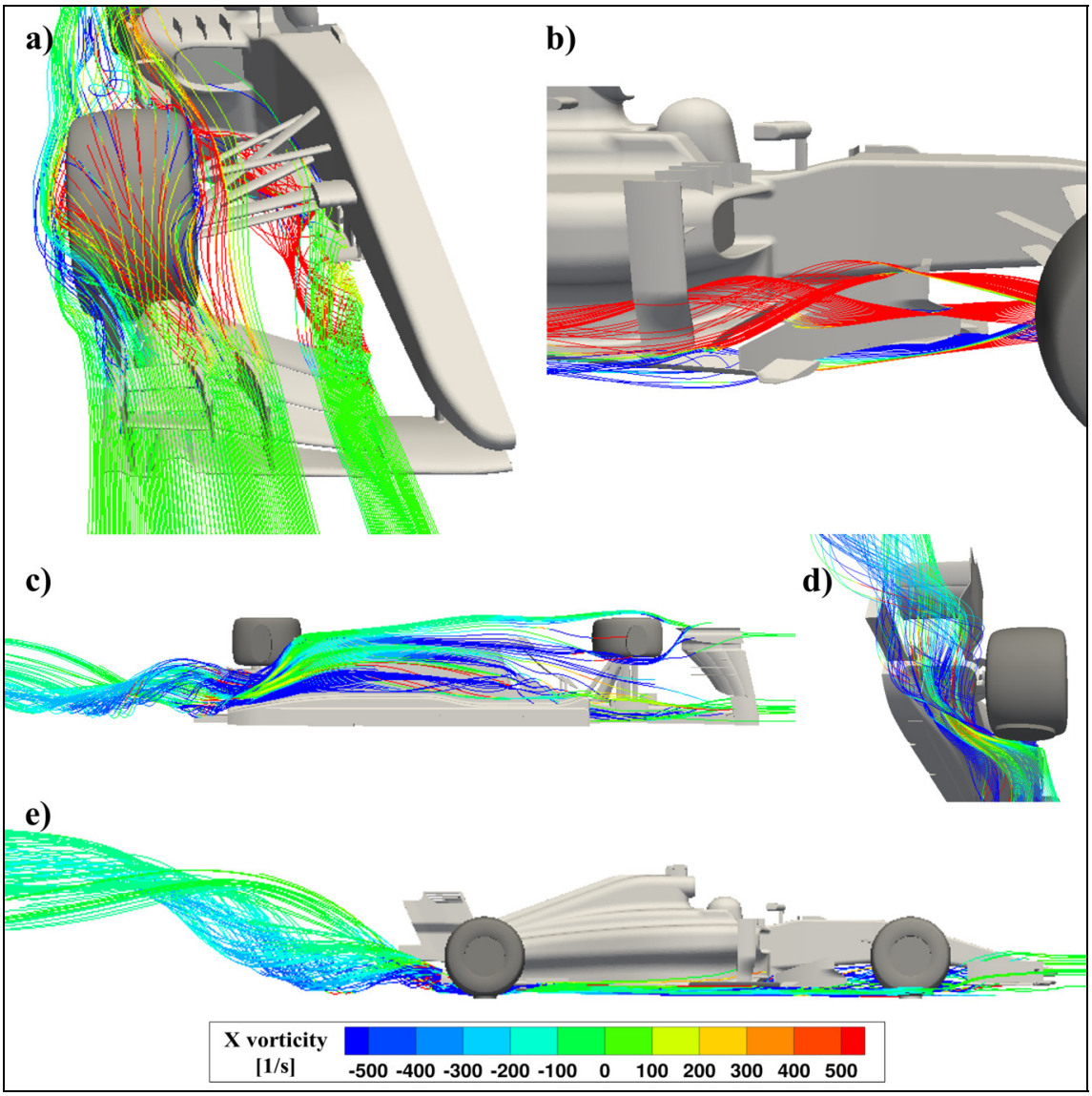

Fig. 7 Streamlines colored by axial vorticity: (a) front wing,; (b) bargeboard; (c) underbody (bottom view); (d) diffuser; (e) underbody (side view).

task of the front wing is best highlighted by Fig. 7a: apart from the primary function of generating downforce, it energizes the flow for better feeding the downstream aerodynamic devices, such as the underfloor.

Fig. 7b puts in evidence the interaction between bargeboard and sidepod panel: the first acts like a huge vortex generator; the latter maintains the energized flow attached to the sides of the vehicle. The downforce generated by the underbody is a direct result of the vehicle front-end design: in fact, the diffuser is partially fed by the flow bypassing the front tires (Fig. 7c). As witnessed by Fig. 7d, the entire underfloor is characterized by highly three-dimensional streamlines strengthened by the diffuser activity: it accelerates the flow at its inlet and creates additional downforce by means of strong vortices. Fig. 7e gives evidence of the diffuser impact on the outflow: the streamlines are deflected upwards, giving rise to a huge wake. Besides the flow coming from the underfloor, the overall wake consists of several contributions, including that of rear wing and rear tires: this explains why a modern F1 car is not able to generate an adequate amount of downforce in

slipstream.

5. Conclusions

Aerodynamic performance of a F1 2017 car designed by PERRINN was analysed by the open-source software OpenFOAM. The meshing phase was particularly tricky because of the sophisticated geometry of the vehicle. SnappyHexMesh, the dedicated OpenFOAM tool, despite some challenges such as the layer addition algorithm, provided a fast and automatic meshing procedure.

In view of the simulation complexity, a coupled approach was chosen to avoid numerical instability in the very first iterations and reduce the number of iterations to reach convergence. The results of the S-A RANS incompressible calculation were found to be in good agreement with the reference data in terms of drag, downforce efficiency and front balance. As a general comment, OpenFOAM is a good instrument for external aerodynamic investigations, considering that it is license-free and it is particularly suitable for parallel computing.

Regarding the F1 car aerodynamics, it can be concluded that the flow field involves slender and blunt bodies interacting with each other. A F1 car generates downforce in different ways: by inverted multi-element wings, ground effect of the underbody, Venturi effect of the diffuser and vorticity management. The contributions of front and rear wing to downforce are 26.3% and 27.5%, respectively; most of the remaining percentage is attributable to the underbody. Front and rear wheels are the main source of pressure drag, because they generate a huge wake. The rear wing is primarily responsible for induced drag, as a result of axial vortices detaching from the wingtips. The front wing deserves a comment of its own: its axial vortices can be used to improve the performance of the underbody and consequently generate more downforce.

It appears that ground effect is the most convenient way to generate downforce: for this reason underbody is more efficient than front wing, and front wing is in turn more efficient than rear wing.

Acknowledgments

We acknowledge the CINECA award under the LISA initiative, for the availability of high performance computing resources and support. Special thanks to Nicolas Perrin and his team for sharing their F1 project.

References

[1] Hanna, R. K. 2012. “CFD in Sport-a Retrospective; 1992-2012.” *Procedia Engineering* 34: 622-7.

[2] Larsson, T., Sato, T., and Ullbrand, B. 2005. “Supercomputing in F1—Unlocking the Power of CFD.” 2nd European Automotive CFD Conference, Frankfurt, Germany.

[3] Zhang, X., Toet, W., and Zerihan, J. 2006. “Ground Effect Aerodynamics of Race Cars.” *Applied Mechanics Reviews* 59.1: 33-49.

[4] Larsson, T. 2009. “Formula One Aerodynamics—BMW Sauber F1.09—Fundamentally Different.” EASC 2009, 4th European Automotive Simulation Conference, Munich, Germany.

[5] Perry, R. L., and Marshall, D. D. 2008. “An Evaluation of Proposed Formula 1 Aerodynamic Regulations Changes Using Computational Fluid Dynamics.” 26th AIAA Applied Aerodynamics Conference, Hawaii.

[6] Nebenführ, B. 2010. “OpenFOAM: A Tool for Predicting Automotive Relevant Flow Fields.” A paper of Chalmers University of Technology.

[7] Islam, M., Decker, F., de Villiers, E., Jackson, A., Gines, J., Grahs, T., Gitt-Gehrke, A., and Comas i Font, J. 2009. “Application of Detached-Eddy Simulation for Automotive Aerodynamics Development.” No. 2009-01-0333, SAE technical paper.

[8] Ravelli, U., and Savini, M. n.d. “Aerodynamic Investigation of Blunt and Slender Bodies in Ground Effect Using OpenFOAM.” Unpublished.

[9] Haller, G. 2005. “An Objective Definition of a Vortex.” *J. Fluid Mech.* 525: 1-26.